

Spectral characteristics of foreshocks preceding major earthquakes of the Kurile-Kamchatka Arc and their application to the prediction of the main shock time

L. S. Chepkunas, E. A. Rogozhin, and V. I. Benikova

Geophysical Survey, Russian Academy of Sciences

Abstract. The spectral analysis of waveforms from moderate and weak earthquakes in the Kurile-Kamchatka region allows one to rather reliably discriminate between foreshocks of forthcoming strong events and independent swarms of seismic shocks. Anomalously high frequencies of seismic radiation from foreshock sources are due to an anomalous rigidity of the seismogenic medium. Based on significant frequency anomalies determined from seismic records of foreshock sequences, the methods developed by the authors can be applied to recognize medium- and short-term seismological precursory effects.

Introduction

Important factors related to the prediction of a strong earthquake are any changes in the seismicity pattern or in seismic waveforms recorded from earthquakes that occur immediately before the main shock. Many authors reported an increase in the number of weak shocks in the vicinity of the forthcoming earthquake epicenter, i.e. the appearance of weak foreshocks shortly before the main earthquake [Ishida and Kanamori, 1980; Mogi, 1988]. As a rule, areas of the foreshock occurrence are tectonically inhomogeneous [Boldyrev, 1987; Goryachev, 1966], and the distribution of foreshock sources is controlled by local tectonic conditions within relatively small geological structures. On the other hand, the development of the main shock source of a major earthquake involves large seismogenic structures and is controlled by a regional stress field. Therefore, although the discrimination between foreshocks and ordinary earthquake swarms encounters considerable difficulties, it is not a basically unsolvable problem. Not all strong earthquakes are preceded by foreshocks. Differences between waveforms of foreshocks and ordinary seismic shocks, as well as their spectral characteristics, were proposed to use for the identification

of foreshocks in [Ishida and Kanamori, 1980; Utsu, 1980], because foreshock seismograms are dominated by higher frequencies, whereas lower-frequency waveforms are characteristic of ordinary weak earthquakes.

We conducted a retrospective analysis of foreshocks preceding two recent strong earthquakes that occurred within the Kurile-Kamchatka arc: Shikotan, October 4, 1994 ($M=8.4$) and Kronotski, December 5, 1997 ($M=7.9$) earthquakes, as recorded at digital IRIS (vertical Z component) stations in Obninsk and Arti. Their sources arose in similar seismotectonic settings within the continental slope of the island arc, in the upper part of the Zavaritskii-Benioff focal zone. We also compared their waveforms with seismic records of several independent ordinary shocks in the same seismotectonic province.

Both earthquakes have been well studied and source parameters of their main shocks have been determined. Their study was supplemented by examination of coseismic deformations and geodetic measurements in the epicentral region [Kronotski Earthquake..., 1998; Shikotan Earthquake..., 1994, 1995]. The structure of the crust and upper mantle beneath the Kurile-Kamchatka arc has been studied in detail by geophysical methods [Rodnikov, 1979; *The Structure of Seismic Focal Zones*, 1987; *The Structure of the Sea of Okhotsk Floor*, 1981; Tarakanov, 1997; Zlobin, 1987]. This provided a rather clear conception of the environment in which the sources of these earthquakes arose and of the structure of their sources.

Structural patterns of the seismic sources and seismogenic media, as well as their stress-strain states, can be helpful to the search for features discriminating between the records of foreshocks and ordinary seismic events.

Copyright 2001 by the Russian Journal of Earth Sciences.

Paper number TJE01064.
ISSN: 1681-1208 (online)

The online version of this paper was published Sep. 28, 2001.
URL: <http://rjes.agu.org/v03/TJE01064/TJE01064.htm>

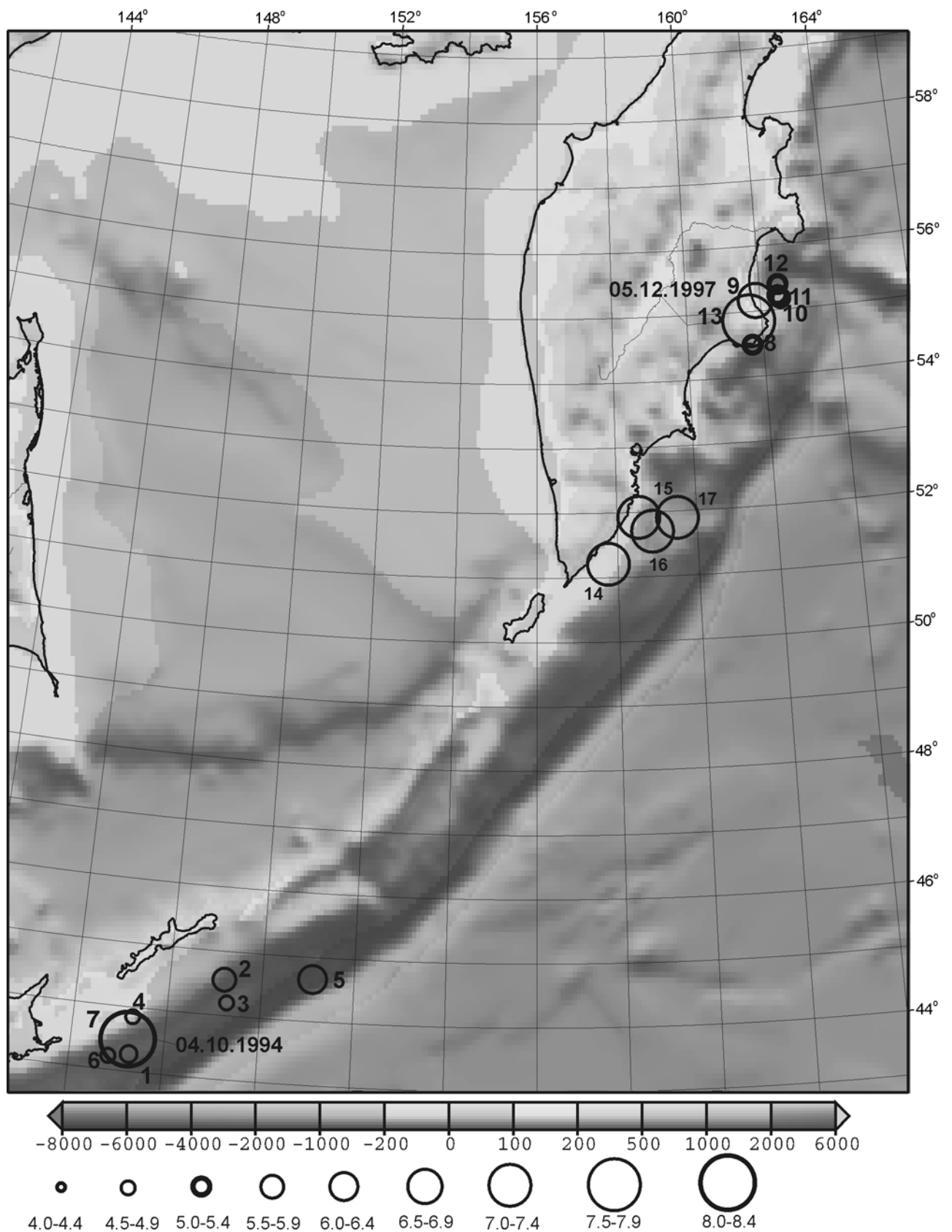


Figure 1. Map showing epicenters of earthquakes.

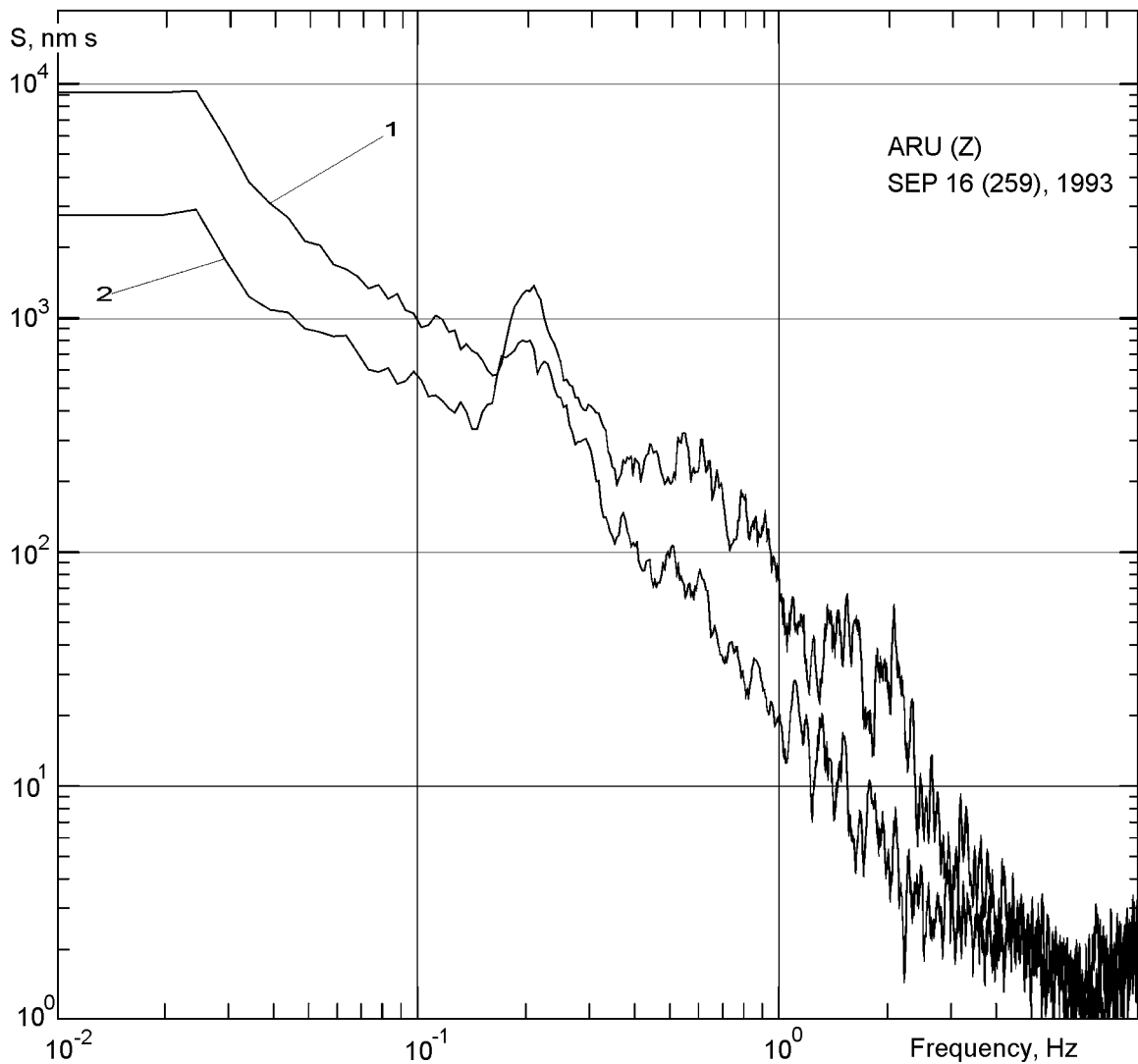


Figure 2. Spectra of P waves and noise from the Arti records of the September 16, 1993 Shikotan earthquake: (1) signal; (2) noise.

Foreshocks of the Shikotan Earthquake

We analyzed spectral parameters of the foreshocks of the Shikotan, October 4, 1994 earthquake, recorded by digital instruments at the Obninsk and Arti stations. The source area bounded by the coordinates 42.3 N, 146.0 E; 42.95 N, 145.4 E; 44.95 N, 148.9 E; 44.6 N, 149.2 E; 42.3 N, 146.0 E was considered.

Foreshocks were defined as $M \geq 5$ earthquakes with focal depths shallower than 70 km that occurred in this area in 1993 and 1994. The records of only six foreshocks (nos. 1–6) and the main shock (no. 7) were found to be suitable for the spectral treatment; their parameters are presented in Table 1 and the map showing their epicenters is given in Figure 1.

The Arti (ARU) and Obninsk (OBN) stations are located at respective distances of 54° and 65° from the epicentral zone. A stable wave pattern is observed at these distances.

The amplitude spectra were calculated with the help of the Service Access Controller (SAC) software, which is an interactive general-purpose program including spectral analysis modules enabling the separation, calculation and analysis of spectral components of the signal.

P wave record intervals 120–140 s long (between the P wave and PP reflection arrivals) were chosen. The noise spectra were also calculated from records obtained before the earthquake. The noise interval analyzed had the same length as the desired signal. The ratio of spectral densities S at different frequencies from a given event was considered as an indicator of a change in the spectral composition of earthquakes preceding the main shock. The station spectra were corrected for the frequency response of instrumentation and were reduced to the source, allowing for the energy loss of traveling P waves due to their geometrical divergence $G(\Delta)$, for the radiation pattern from the source $R\theta\varphi$, inelastic attenuation $m(f)$, and the frequency response effect of the

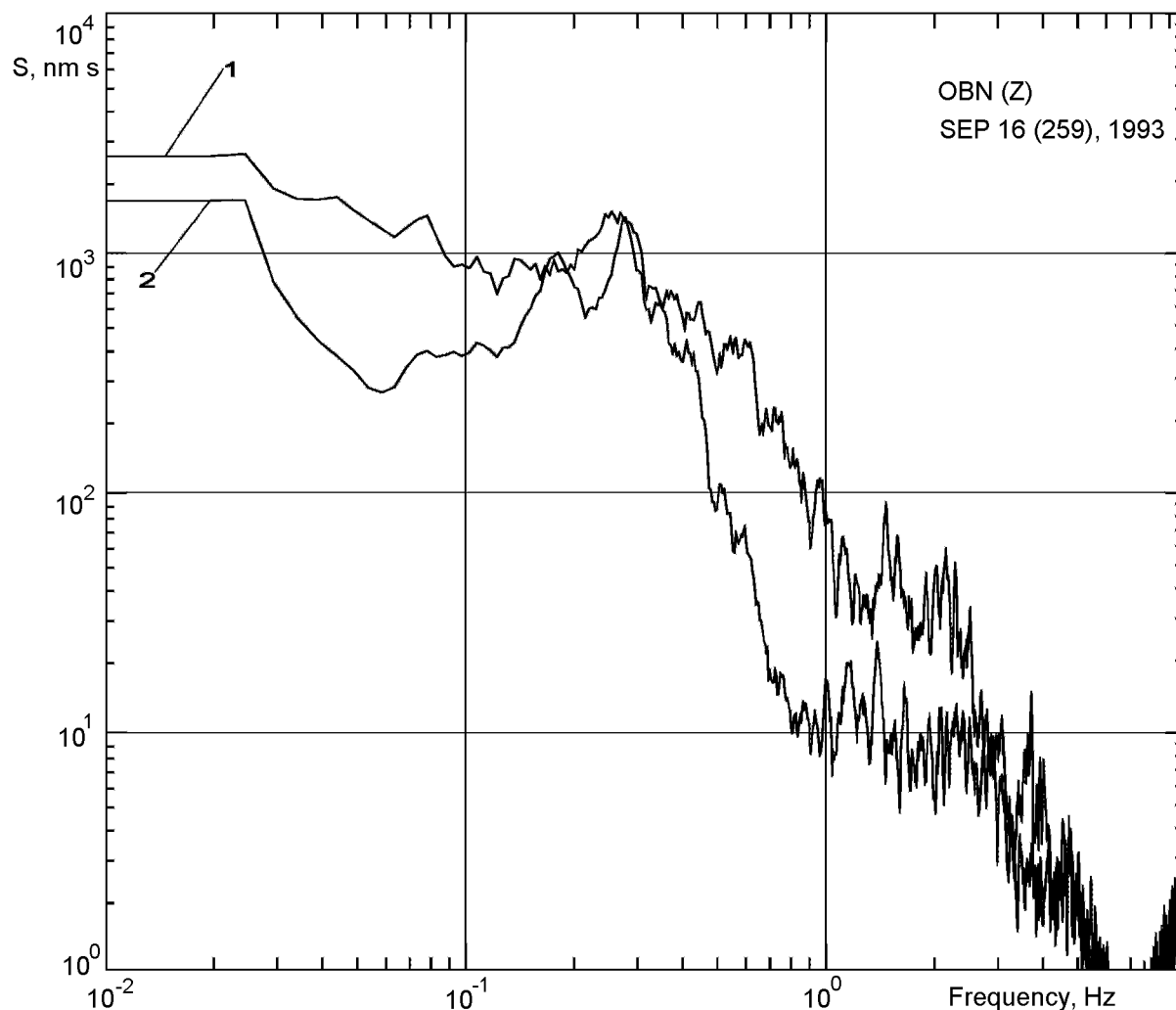


Figure 3. Spectra of P waves and noise from the Obninsk records of the September 16, 1993 Shikotan earthquake: (1) signal; (2) noise.

crust under the station $c(f)$ [Aptekman *et al.*, 1989]. The first two factors are frequency independent and only modify the spectrum level, whereas the two other effects rearrange the entire spectral picture (appearance).

The spectra of the noise and desired signals were first

compared in order to choose the interval of frequencies to be analyzed. Figures 2 and 3 present the spectra of P waves and noise from the September 16, 1993 foreshock recorded at the Arti and Obninsk stations; the spectra were corrected for the instrumental frequency response. An amplitude peak

Table 1. Main parameters of foreshocks and the main shock of the Shikotan, October 4, 1994, earthquake

| No. | | | Coordinates | | | Magnitudes | |
|-----|--------------------|-------|---------------------|---------------------|----------|------------|------|
| | Date | h:min | φ° , N | λ° , E | H , km | MS | MPSP |
| 1. | April 17, 1993 | 03:43 | 43.17 | 147.33 | 43 | | 5. |
| 2. | September 16, 1993 | 00:59 | 44.56 | 149.03 | 43 | 5.5 | 6.2 |
| 3. | February 15, 1994 | 23:46 | 44.18 | 149.12 | 5 | 4.8 | 5.6 |
| 4. | June 25, 1994 | 08:38 | 43.91 | 147.31 | 66 | 4.7 | 6. |
| 5. | August 20, 1994 | 04:38 | 44.63 | 149.03 | 41 | 6.3 | 6.8 |
| 6. | September 11, 1994 | 23:20 | 43.16 | 146.97 | 35 | 4.5 | 5.4 |
| 7. | October 4, 1994 | 13:22 | 43.59 | 147.25 | 50 | 8.4 | 7.6 |

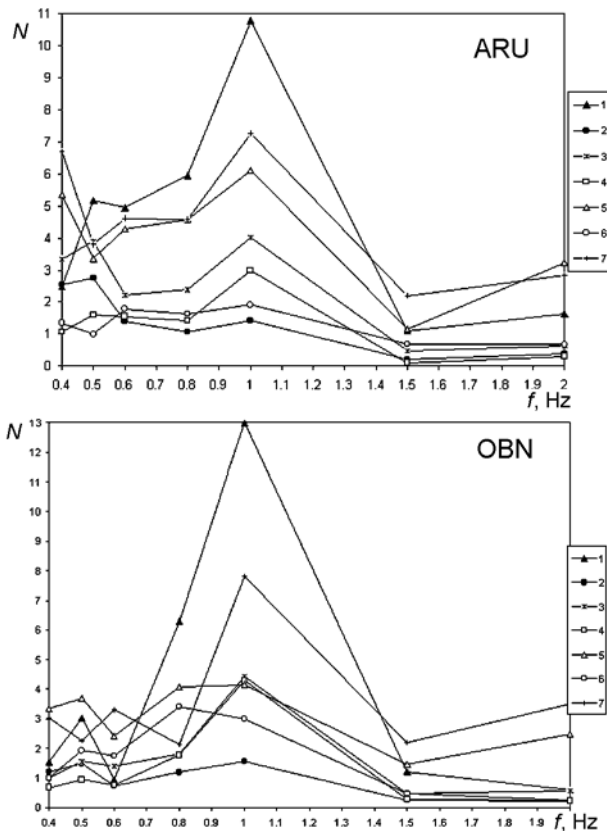


Figure 4. Ratio(N) of spectral amplitudes reduced to source (Shikotan earthquakes).

observed in the ARU and OBN spectra at a frequency of 0.2 Hz (5 s) is evidence of strong microseisms of marine (oceanic) origin. For this reason, the frequency interval $0.13 < f < 0.37$ Hz was excluded from the analysis of spectral amplitudes.

We considered the ratios N of the spectral density S_2 at $f = 0.1$ Hz to the spectral densities $S_3, S_4, S_5, S_6, S_7, S_8$ and S_9 at the respective frequencies $f_3=0.4, f_4=0.5, f_5=0.6, f_6=0.8, f_7=1.0, f_8=1.5$ and $f_9=2.0$ Hz: $N_3 = S_2/S_3, N_4 = S_2/S_4, N_5 = S_2/S_5, N_6 = S_2/S_6, N_7 = S_2/S_7, N_8 = S_2/S_8$ and $N_9 = S_2/S_9$. Average spectral amplitudes were calculated as arithmetical means with given

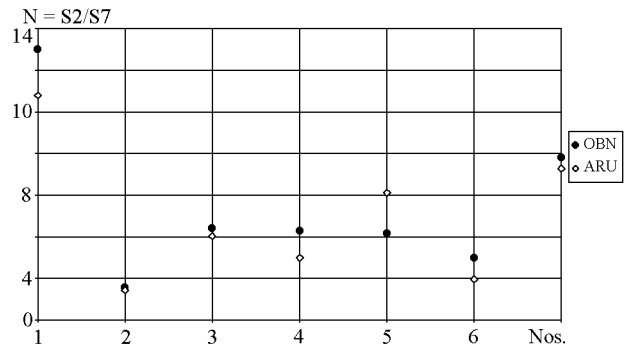


Figure 5. Ratio $N=S_2/S_7$ for Shikotan earthquakes (see Table 1 for the foreshock numbers).

upper and lower boundaries of f ; the respective frequency intervals were 0.8–0.12 Hz for S_2 ($f = 0.1$ Hz), 0.38–0.42 Hz for S_3 (0.4 Hz), 0.48–0.52 for S_4 (0.5 Hz), 0.58–0.62 Hz for S_5 (0.6 Hz), 0.78–0.82 Hz for S_6 (0.8 Hz), 0.95–1.05 Hz for S_7 (1.0 Hz), 1.45–1.55 Hz for S_8 (1.5 Hz) and 1.95–2.05 Hz for S_9 (2.0 Hz).

Tables 2 and 3 present the N values from the ARU and OBN stations.

Based on these data we analyzed the behavior of N at various spectral frequencies for these earthquakes (Figure 4). The highest N values, as constrained by both ARU and OBN records, are observed for shock no. 1 (April 17, 1993; MPSP = 5), the earliest with respect to the main shock; other shocks with similar magnitudes have smaller values of N . For all foreshocks, the N values tend to increase in a 0.6–1.0-Hz interval. With an increase in frequency from 1.0 to 2.0 Hz, N gradually decreases and reaches a minimum at frequencies of 1.5 to 2.0 Hz (Table 3). High N values are also characteristic of earthquake no. 5 ($M = 6.3$) and of the main shock ($M = 8.4$). However, in a 1.5–2.0-Hz interval, N increases for strong earthquakes and decreases for shocks nos. 2–4 and 6.

Therefore, we may suggest that the high-frequency spectral foreshock amplitudes increase toward the onset time of the main shock, which is particularly evident from the N behavior at $f=1.0$ Hz: maximum values of N are observed at this frequency for all events considered (Figure 5). In the case of event no. 1 (April 17, 1993), the high-frequency con-

Table 2. The ratios N of spectral densities for foreshocks and the main shock of the Shikotan earthquake from ARU records (including corrections $m(f)$ and $c(f)$)

| No. | $N_3=S_2/S_3$ | $N_4=S_2/S_4$ | $N_5=S_2/S_5$ | $N_6=S_2/S_6$ | $N_7=S_2/S_7$ | $N_8=S_2/S_8$ | $N_9=S_2/S_9$ |
|-----|--------------------|--------------------|--------------------|--------------------|------------------|--------------------|------------------|
| 1 | 2.5 | 5.2 | 5.0 | 6.0 | 11 | 1.1 | 1.6 |
| 2 | 2.5 | 2.7 | 1.4 | 1.1 | 1.4 | 0.2 | 0.4 |
| 3 | 3.3 | 3.9 | 2.2 | 2.4 | 4.0 | 0.5 | 0.6 |
| 4 | 1.1 | 1.6 | 1.6 | 1.4 | 3.0 | 0.1 | 0.3 |
| 5 | 5.4 | 3.4 | 4.3 | 4.6 | 6.1 | 1.2 | 3.2 |
| 6 | 1.3 | 1.0 | 1.8 | 1.6 | 1.9 | 0.7 | 0.7 |
| 7 | 6.7 | 3.8 | 4.6 | 4.6 | 7.3 | 2.2 | 2.8 |
| | $f(\text{Hz})=0.4$ | $f(\text{Hz})=0.5$ | $f(\text{Hz})=0.6$ | $f(\text{Hz})=0.8$ | $f(\text{Hz})=1$ | $f(\text{Hz})=1.5$ | $f(\text{Hz})=2$ |

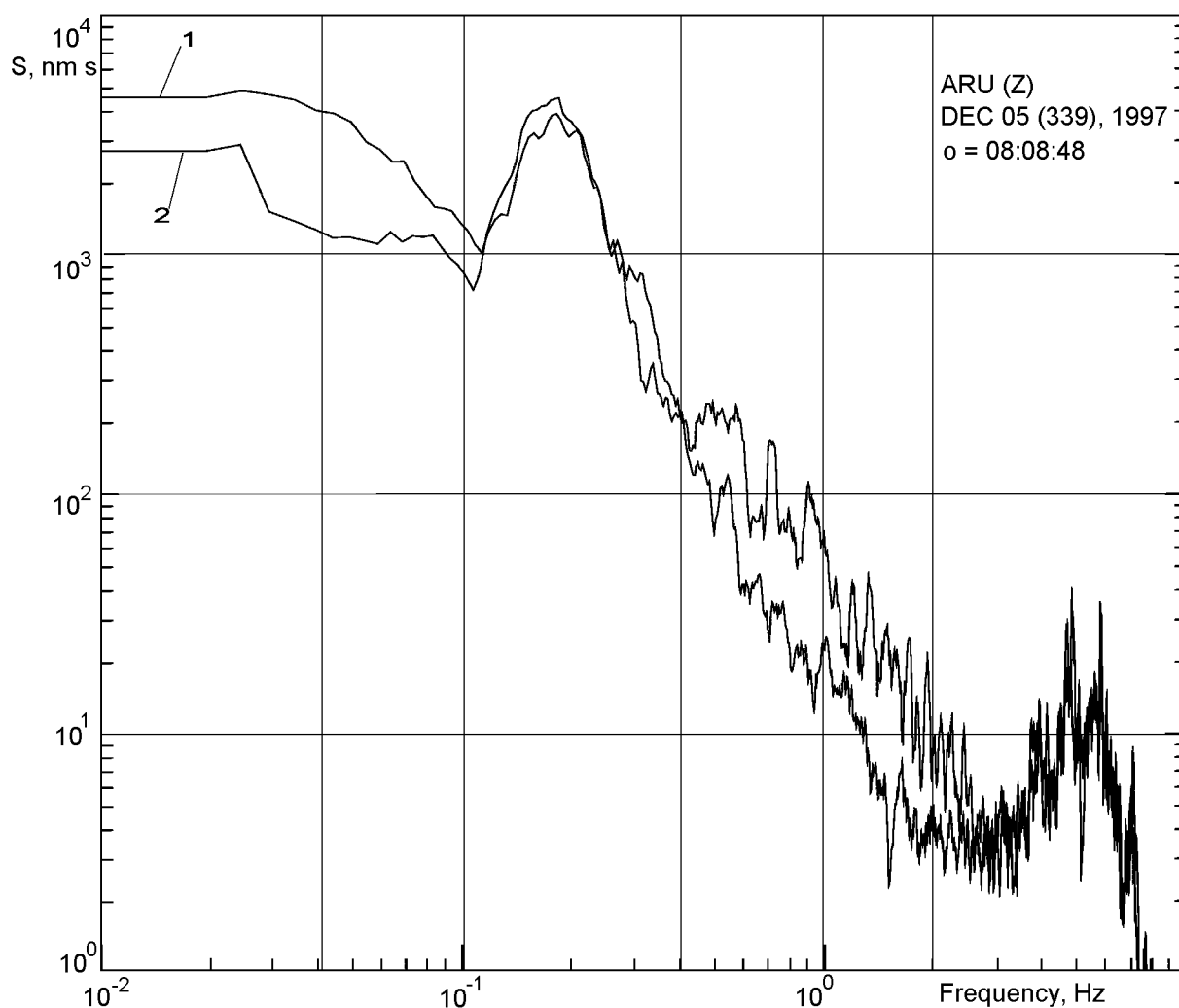


Figure 6. Spectra of P waves and noise from the Arti records of the (08:08) December 5, 1997, Kronotski earthquake: (1) signal; (2) noise.

tribution is small and N values are rather large; however, they decrease toward the time of the main shock and rise immediately before this time moment. The April 17, 1993, earthquake is likely to be an ordinary event rather than a foreshock of the Shikotan earthquake.

Foreshocks of the Kronotski Earthquake

Spectral parameters characterizing foreshocks of the December 5, 1997, Kronotski earthquake that had magnitudes

Table 3. The ratios N of spectral densities for foreshocks and the main shock of the Shikotan earthquake from OBN records (including corrections $m(f)$ and $c(f)$)

| No. | $N_3=S_2/S_3$ | $N_4=S_2/S_4$ | $N_5=S_2/S_5$ | $N_6=S_2/S_6$ | $N_7=S_2/S_7$ | $N_8=S_2/S_8$ | $N_9=S_2/S_9$ |
|-----|--------------------|--------------------|--------------------|--------------------|------------------|--------------------|------------------|
| 1 | 1.5 | 3.0 | 1.0 | 6.3 | 13 | 1.2 | 0.6 |
| 2 | 1.2 | 1.6 | 0.7 | 1.2 | 1.6 | 0.2 | 0.2 |
| 3 | 1.0 | 1.5 | 1.4 | 1.8 | 4.4 | 0.5 | 0.6 |
| 4 | 0.7 | 0.9 | 0.8 | 1.8 | 4.2 | 0.3 | 0.2 |
| 5 | 3.3 | 3.7 | 2.4 | 4.1 | 4.2 | 1.5 | 2.5 |
| 6 | 1.0 | 1.9 | 1.7 | 3.4 | 3.0 | 0.5 | 0.2 |
| 7 | 3.0 | 2.3 | 3.3 | 2.1 | 7.8 | 2.2 | 3.5 |
| | $f(\text{Hz})=0.4$ | $f(\text{Hz})=0.5$ | $f(\text{Hz})=0.6$ | $f(\text{Hz})=0.8$ | $f(\text{Hz})=1$ | $f(\text{Hz})=1.5$ | $f(\text{Hz})=2$ |

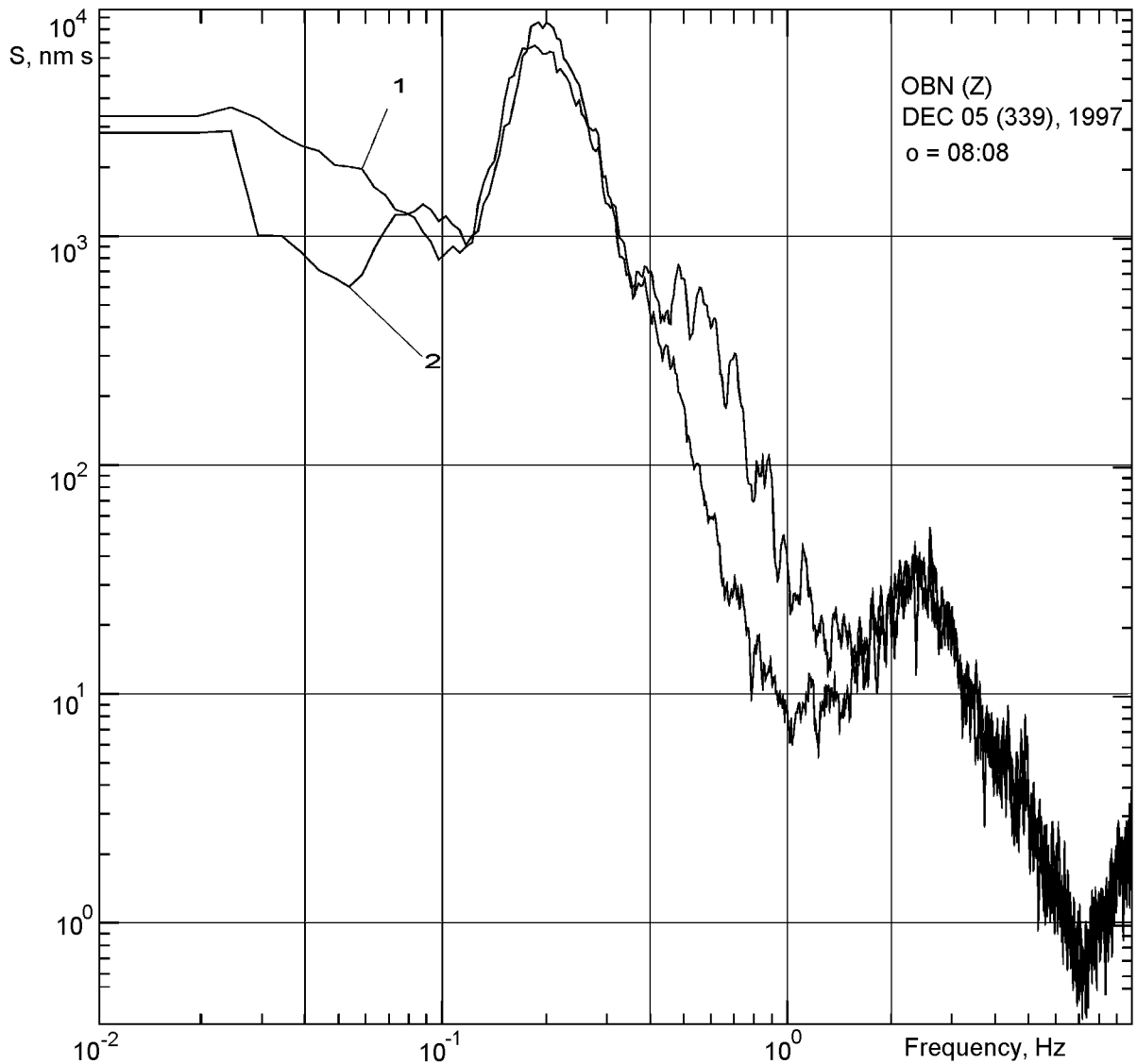


Figure 7. Spectra of P waves and noise from the Obninsk records of the (08:08) December 5, 1997, Kronotski earthquake: (1) signal; (2) noise.

≥ 5 and occurred from 1996 through 1997 in the Kronotski source area (54.1 N, 161.3 E; 54.35 N, 160.8 E; 55.65 N, 162.7 E; 55.4 N, 163.2 E; 54.1 N, 161.3 E) were analyzed so as in the case of the Shikotan earthquake.

Out of eight chosen earthquakes, six events recorded at the Obninsk station and five events recorded at the Arti station were suitable for spectral analysis. The ARU and OBN records of the February 8, 1997, $M = 5.0$ earthquake (07:40) were weak; the spectrum of the December 4, 1997, earthquake (22:41) could only be constructed from OBN records because ARU records included strong microseism noise; and the record of the December 4, 1997, earthquake (22:46) overlapped the record of the preceding seismic shock. Table 4 presents data on the earthquakes used (their enumeration continues Table 1) and their epicenters are shown in Figure 1.

Records from the same digital stations in Arti and Ob-

ninsk, located at respective epicentral distances of 53° and 61.5° , were analyzed. As in the case of the Shikotan earthquake, spectra were calculated using the SAC software. Intervals 130–150 s long between P and PP waves were chosen. Figures 6 and 7 present the December 5, 1997, earthquake (08:08) spectra of P waves and noise corrected for the frequency response of instruments at the Arti and Obninsk stations. As before, all spectra exhibit an amplitude peak at 0.2 Hz (5 s).

As well as in the case of the Shikotan earthquake, the N value is used as a measure of variations in the spectral composition, associated with the forthcoming main shock (Tables 5 and 6).

The N dependences at various spectral frequencies are plotted in Figure 8 for the earthquakes chosen. Note that the N variations associated with the Kronotski and Shikotan earthquakes are similar. Figure 9 shows that the high-

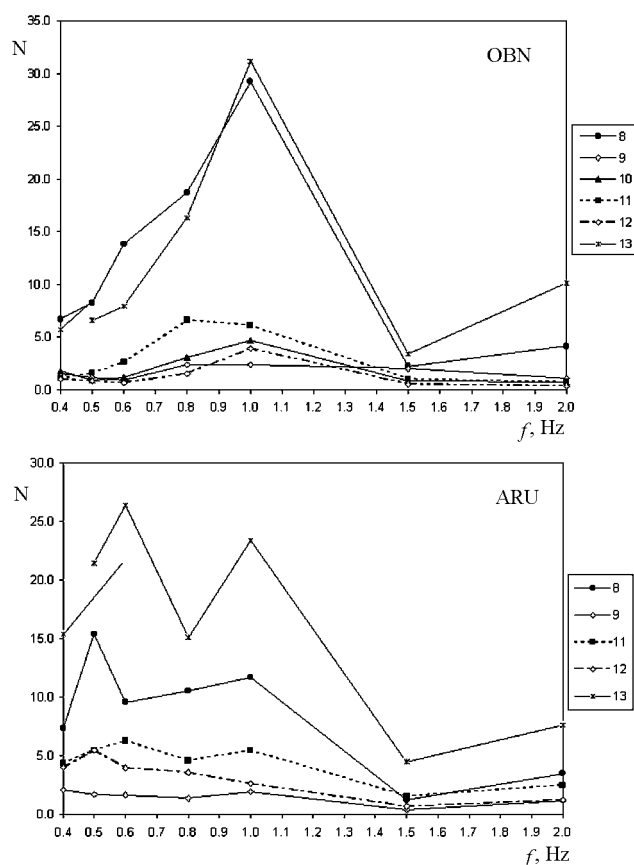


Figure 8. Ratio (N) of spectral amplitudes reduced to source (Kronotski earthquakes).

frequency contribution to the spectra is initially small (August 5, 1996, earthquake) and N values are fairly large; the foreshock values of N decrease with time but rise again immediately before the main shock and reach a maximum. The August 5, 1996, earthquake is likely to have been an ordinary event rather than a foreshock of the Kronotski earthquake.

As examples of ordinary events, we considered four Kamchatka earthquakes that occurred in a different area from 1993 through 1999 (Table 7) and that can by no means be regarded as foreshocks of stronger events.

Tables 8 and 9 present spectral densities N for these earthquakes. As seen from these tables, the N values of the

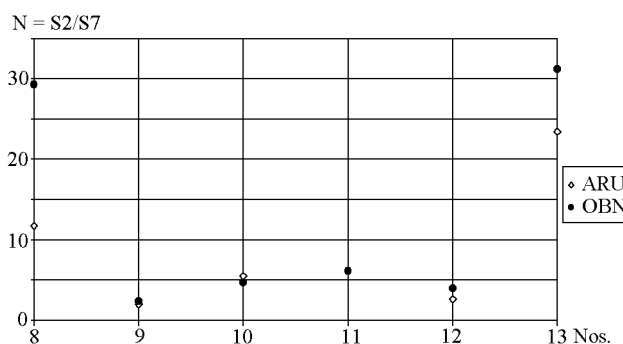


Figure 9. Ratio $N=S2/S7$ for Kronotski earthquakes (see Table 4 for the foreshock numbers).

ordinary earthquakes are close to those obtained from the main shock of December 5, 1997 and from the earthquake of August 5, 1996 classified here as an ordinary event. The patterns of the N variation with frequency are also similar. Consequently, earthquakes nos. 14–17 can also be classified as ordinary events.

Discussion of the Results

The above data suggest that the development of a strong earthquake source is accompanied by significant variation in the frequency composition of seismic radiation from moderate earthquakes that occur in the source area of the forthcoming strong event. About one year before the strong earthquake, seismic records of such relatively weak earthquakes become enriched in higher frequencies, which is untypical of independent strong events (in our case, the Shikotan and Kronotski main shocks), as well as of moderate and weak ordinary earthquakes. On the other hand, relatively weak independent shocks that occur inside or outside source zones of forthcoming strong earthquakes are similar in lower-frequency bias of their seismic radiation. These variations in seismic records are reliably resolved by the spectral analysis of digital seismograms. Since the procedure of the spectral analysis of waveforms can be automated, it is possible in the near future to conduct medium-term monitoring of potential strong earthquakes source zones that are assessed to be hazardous from data of long-term prediction methods.

Table 4. Main parameters of foreshocks and the main shock of the Kronotski, December 5, 1997, earthquake

| No. | | | Coordinates | | | Magnitudes | |
|-----|------------------|-------|---------------------|---------------------|----------|------------|------|
| | Date | h:min | φ° , N | λ° , E | H , km | MS | MPSP |
| 8. | August 5, 1996 | 00:25 | 54.58 | 161.77 | 33 | 5.1 | 5.2 |
| 9. | February 9, 1997 | 18:57 | 55.14 | 161.96 | 65 | 5.6 | 6.3 |
| 10. | December 4, 1997 | 22:41 | 55.18 | 162.56 | 38 | 5.4 | 5.4 |
| 11. | December 5, 1997 | 00:06 | 55.20 | 162.48 | 33 | 5.0 | 5.1 |
| 12. | December 5, 1997 | 08:08 | 55.33 | 162.51 | 22 | 5.6 | 5.4 |
| 13. | December 5, 1997 | 11:26 | 54.88 | 161.95 | 33 | 7.9 | 7.0 |

Table 5. Spectral density ratios N for foreshocks and the main shock of the Kronotski earthquake from ARU records (including corrections $m(f)$ and $c(f)$)

| No. | $N3=S2/S3$ | $N4=S2/S4$ | $N5=S2/S5$ | $N6=S2/S6$ | $N7=S2/S7$ | $N8=S2/S8$ | $N9=S2/S9$ |
|-----|--------------------|--------------------|--------------------|--------------------|--------------------|--------------------|--------------------|
| 8 | 7.4 | 9.9 | 9.6 | 11 | 12 | 1.2 | 3.5 |
| 9 | 2.1 | 1.7 | 1.7 | 1.4 | 2.0 | 0.4 | 1.2 |
| 11 | 4.4 | 5.5 | 6.3 | 4.6 | 5.5 | 1.5 | 2.5 |
| 12 | 4.0 | 5.5 | 4.0 | 3.6 | 2.6 | 0.7 | 1.2 |
| 13 | 15 | 15 | 16 | 17 | 23 | 4.5 | 7.6 |
| | $f(\text{Hz})=0.4$ | $f(\text{Hz})=0.5$ | $f(\text{Hz})=0.6$ | $f(\text{Hz})=0.8$ | $f(\text{Hz})=1.0$ | $f(\text{Hz})=1.5$ | $f(\text{Hz})=2.0$ |

Table 6. Spectral density ratios N for foreshocks and the main shock of the Kronotski earthquake from ARU records (including corrections $m(f)$ and $c(f)$)

| No. | $N3=S2/S3$ | $N4=S2/S4$ | $N5=S2/S5$ | $N6=S2/S6$ | $N7=S2/S7$ | $N8=S2/S8$ | $N9=S2/S9$ |
|-----|--------------------|--------------------|--------------------|--------------------|--------------------|--------------------|--------------------|
| 8 | 6.7 | 8.3 | 14 | 19 | 29 | 2.3 | 4.1 |
| 9 | 1.5 | 1.2 | 0.9 | 2.4 | 2.3 | 2.0 | 1.1 |
| 10 | 1.7 | 0.9 | 1.2 | 3.1 | 4.7 | 0.8 | 0.7 |
| 11 | 1.1 | 1.6 | 2.6 | 6.6 | 6.1 | 1.0 | 0.7 |
| 12 | 1.0 | 0.8 | 0.7 | 1.5 | 3.9 | 0.5 | 0.4 |
| 13 | 5.7 | 6.6 | 7.9 | 16 | 31 | 3.4 | 10 |
| | $f(\text{Hz})=0.4$ | $f(\text{Hz})=0.5$ | $f(\text{Hz})=0.6$ | $f(\text{Hz})=0.8$ | $f(\text{Hz})=1.0$ | $f(\text{Hz})=1.5$ | $f(\text{Hz})=2.0$ |

Thus, the spectral analysis of waveforms can be used as a reliable, medium- to short-term seismological precursor of the occurrence time of strong earthquakes.

The Seismotectonic Origin of Seismic Radiation Frequency Anomalies Characteristic of Foreshock Sequences

According to fault plane solutions and results of studying the aftershock process, the sources of the strongest earthquakes that occurred on the continental slope of the Kurile-Kamchatka arc from 1994 through 1997 can be divided into two types. The first type includes thrust motions on planes gently dipping west or northwest under island arcs. Epicentral zones of this type of sources (e.g., the source of the Kronotski, $M = 7.9$, earthquake of December 5, 1997 in the east of Kamchatka) were oriented parallel to the island arc and were located on the continental (near-island) slope of the island arc. They are most conformable to the notion

of “interplate” earthquakes [Rogozhin and Zakharova, 1998]. Their source motions can be directly associated with the Pacific plate subduction under the island arc.

The second type of seismic sources is characteristic of “intraplate” earthquakes [Rogozhin and Zakharova, 1998]. These shallow earthquakes also occur under the near-island slope, on the northwestern slope of the Kurile-Kamchatka deep-sea trench. The fault planes of these seismic events (e.g., Shikotan, South Kuriles, $M = 8.4$ earthquake of October 4, 1994 [Zakharova et al., 1997, 1998]) are oriented parallel to the island arc and steeply dip eastward (or southeastward) beneath the deep-sea trench. The seismogenic slip in the Shikotan source was a reversed fault with a minor right-lateral component; as a result, the lower islandward portion of the slope was thrown up relative to its upper portion. Since the source of such a strong earthquake is very large, it penetrated through the entire lithosphere and cut the Benioff zone throughout its thickness. Seismic sources of such type by no means fit the concept of seismicity induced by the subduction process.

The reconstruction of the regional stress field from seismo-

Table 7. Ordinary earthquakes in Kamchatka

| No. | Coordinates | | | | | Magnitudes | |
|-----|-------------------|-------|---------------------|---------------------|----------|------------|------|
| | Date | h:min | φ° , N | λ° , E | H , km | MS | MPSP |
| 14. | June 8, 1993 | 13:03 | 51.25 | 157.77 | 54 | 7.4 | 6.5 |
| 15. | November 13, 1993 | 01:18 | 51.95 | 158.67 | 52 | 7.1 | 6.5 |
| 16. | June 21, 1996 | 13:57 | 51.79 | 158.98 | 36 | 7.3 | 6.6 |
| 17. | March 8, 1999 | 12:25 | 52.07 | 159.37 | 33 | 7.1 | 6.1 |

Table 8. Spectral density ratios N for the ordinary earthquakes from ARU records

| No. | $N3=S2/S3$ | $N4=S2/S4$ | $N5=S2/S5$ | $N6=S2/S6$ | $N7=S2/S7$ | $N8=S2/S8$ | $N9=S2/S9$ |
|-----|--------------------|--------------------|--------------------|--------------------|--------------------|--------------------|--------------------|
| 14. | 7.4 | 6.1 | 9.9 | 10 | 11 | 2.2 | 5.5 |
| 15. | 6.7 | 8.3 | 6.9 | 11 | 8.7 | 3.2 | 6.2 |
| 16. | 14 | 23 | 16 | 22 | 27 | 4.2 | 12 |
| | $f(\text{Hz})=0.4$ | $f(\text{Hz})=0.5$ | $f(\text{Hz})=0.6$ | $f(\text{Hz})=0.8$ | $f(\text{Hz})=1.0$ | $f(\text{Hz})=1.5$ | $f(\text{Hz})=2.0$ |

logical data at the eastern Asian margin shows that its principal compression axis is oriented across the island arc strike and gently dips toward the deep-sea trench [Balakina, 1995; Zakharova et al., 1997, 1998]. The extension axis steeply dips oceanward. With such an orientation of stress axes, the shear planes are intersecting surfaces parallel to the island arc; one of these planes gently dips under the arc and is a nearly pure thrust of the island arc over the trench, whereas the other is a reversed fault steeply dipping under the trench and displacing lower part of the slope upward relative to its upper part. On the near-island slope, these planes are conformable to geological structures revealed from geomorphological observations and seismic studies (common reflection point, continuous seismic profiling, deep seismic sounding and reflection methods). On the one hand, this is a large thrust with a displacement amplitude of up to 60 km gently dipping arcward and juxtaposing the crystalline rocks underlying the near-island slope and loose sedimentary rocks of the trench [The Structure of the Sea of Okhotsk Floor, 1981; Udintsev, 1972]. On the other hand, the aforementioned counterpart structures are represented by a series of steep eastward-dipping reversed faults expressed in the submarine slope topography as several subparallel ridges with acoustic basement rocks cropping out among loose sediments. Fault planes in sources of inter- and intraplate earthquakes of the island arc are associated exactly with these structures [Rogozhin and Zakharova, 1998, 2000; Zakharova et al., 1997, 1998].

Moreover, these two types of crosswise sources under the near-island slope are interrelated. A subvertical reversed fault hinders the free motion on a deep thrust plane. The arising barrier is overcome by an interplate earthquake which gives rise to a new seismic barrier, this time hindering the free relative motion of the reversed fault walls. Afterward, this barrier in turn is overcome by an intraplate earthquake. These motion types often rapidly replace one another in sources of the same area. Thus, the main shock of the Shikotan earthquake was of the intraplate type, and the source motion of its strongest aftershock that occurred a few days later can be classified as belonging to the interplate type

[Zakharova et al., 1997, 1998]. On the other hand, the focal mechanism of the Kronotski earthquake is consistent with a thrust on the continental slope, with rock masses moving from the arc oceanward; i.e. the main shock in this case was of the interplate type, and the strong aftershock of the same day was of the intraplate type, as is evident from its focal mechanism [Kronotski Earthquake..., 1998; Rogozhin and Zakharova, 2000].

The existence of the barrier hindering free motions of lithospheric blocks on low- or high-angle major faults significantly changes the stress-strain state of the geological medium in an area of a forthcoming strong earthquake. The medium becomes more rigid and stronger. Moderate and weak earthquakes that occur in the area of a forthcoming strong shallow earthquake (foreshocks) are associated not with the aforementioned major seismogenic structures but with local faults, often randomly oriented relative to the principal axes of the regional stress field. This accounts for significant anomalies in seismogenic source motions of such weak and moderate events (atypical fault plane solutions and high-frequency bias in seismic records as compared with "ordinary" independent background events).

The overcoming of the seismic barrier in the main shock process restores for a time the mobility of major faults of either interplate or intraplate type and removes anomalous motion patterns in sources of the main shock and its aftershocks. Therefore, seismological manifestations of these events are similar in their characteristics to those of "independent" moderate and weak earthquakes and are a natural consequence of main tendencies in the seismotectonic process realized as seismogenic slips on faults of general system of fractures in an undisturbed regional stress field.

Conclusion

Our study showed that the spectral analysis of waveforms of moderate and weak earthquakes in the Kurile-Kamchatka region allows one to reliably discriminate between the foreshocks of forthcoming strong events and independent swarms

Table 9. Spectral density ratios N for the ordinary earthquakes from OBN records

| No. | $N3=S2/S3$ | $N4=S2/S4$ | $N5=S2/S5$ | $N6=S2/S6$ | $N7=S2/S7$ | $N8=S2/S8$ | $N9=S2/S9$ |
|-----|--------------------|--------------------|--------------------|--------------------|--------------------|--------------------|--------------------|
| 14. | 6.7 | 6.1 | 12 | 11 | 14 | 3.2 | 6.4 |
| 16. | 7.4 | 14 | 13.5 | 24 | 34 | 2.7 | 9.8 |
| 17 | 5.5 | 11 | 16 | 26 | 52 | 7.0 | 14 |
| | $f(\text{Hz})=0.4$ | $f(\text{Hz})=0.5$ | $f(\text{Hz})=0.6$ | $f(\text{Hz})=0.8$ | $f(\text{Hz})=1.0$ | $f(\text{Hz})=1.5$ | $f(\text{Hz})=2.0$ |

of seismic shocks. A higher-frequency bias in the seismic radiation from foreshock sources is due to the anomalously rigid state of the seismogenic medium associated with the existence of a barrier that hinders free motions on major fault planes. Based on significant frequency anomalies in seismic records of foreshock sequences, the techniques developed in our study can be used for the recognition of medium- and short-term precursory seismological effects.

Acknowledgments. This work was supported by the Russian Foundation for Basic Research (project no. 99-05-64582), the International Science and Technology Center (project no. 1121) and the Ministry of Industry, Science and Technology of the Russian Federation (International Russian-Japanese project "Seismotectonics of the Russian Far East").

References

- Aptekman, Zh. Ya., Yu. F. Belavina, A. I. Zakharova, et al., Application of *P* wave spectra to the determination of dynamic parameters of earthquake sources: The station-to-source spectrum transition and calculation of dynamic source parameters, *Vulkanol. Seismol.*, (2), 66–79, 1989 (in Russian).
- Balakina, L. M., Kurile-Kamchatka seismogenic zone: The structure and earthquake generation pattern, *Fiz. Zemli*, (12), 48–57, 1995 (in Russian).
- Boldyrev, S. A., Seismological inhomogeneities of active oceanic margins and their tectonic implications, in *Structure of Seismic Focal Zones*, p. 189–198, Nauka, Moscow, 1987 (in Russian).
- Goryachev, A. V., *Main Characteristics of the Tectonic Development of the Kurile-Kamchatka Zone*, Nauka, Moscow, 1966 (in Russian).
- Ishida, M., and H. Kanamori, Temporal variation of seismicity and spectrum of small earthquakes preceding the 1952 Kern County, California earthquake, *Bull. Seismol. Soc. Am.*, 70, 509–527, 1980.
- Kronotski Earthquake of December 5, 1997 in Kamchatka: Precursors, Peculiarities and Consequences*, 294 pp., KGARF, Petropavlovsk-Kamchatski, 1998 (in Russian).
- Mogi, K., *Prediction of Earthquakes*, Mir, Moscow, 1988 (in Russian).
- Rodnikov, A. G., *Eastern Pacific Island Arcs*, Nauka, Moscow, 1979 (in Russian).
- Rogozhin, E. A., and A. I. Zakharova, Tectonic origin of the seismic activation of 1994–1996 at the eastern active margin of Asia, in *Tectonics and Geodynamics: General and Regional Aspects (Conf. Proc.)*, vol. 2, p. 118–121, Geos, Moscow, 1998 (in Russian).
- Rogozhin, E. A., and A. I. Zakharova, Geodynamic position of the Kronotski, eastern Kamchatka earthquake of 1997, *Fiz. Zemli*, (5), 22–27, 2000 (in Russian).
- Shikotan Earthquake of October 4(5), 1994*, *Inf. Analit. Byull. FSSNPG*, extra issue, 1994 (in Russian).
- Shikotan Earthquake of 1994*, *Inf. Analit. Byull. FSSNPG*, special issue, edited by S. S. Aref'ev and N. V. Shebalin, 1995 (in Russian).
- Tarakanov, R. Z., *The Velocity Structure of the Upper Mantle in the Asia-to-Pacific Transition Zone*, (Preprint), Yuzhno-Sakhalinsk, 1997 (in Russian).
- The Crust of Island Arcs and Far East Seas*, Nauka, Moscow, 1972 (in Russian).
- The Structure of Seismic Focal Zones*, Nauka, Moscow, 1987 (in Russian).
- The Structure of the Sea of Okhotsk Floor*, Nauka, Moscow, 1981 (in Russian).
- Udintsev, G. B., *Geomorphology and Tectonics of the Pacific Ocean Floor*, Nauka, Moscow, 1972 (in Russian).
- Utsu, T., Spatial and temporal distribution of low-frequency earthquakes in Japan, *J. Phys. Earth*, 28, 361–384, 1980.
- Zakharova, A. I., S. G. Poigina, E. A. Rogozhin, and O. E. Starovoit, Earthquakes in Eurasia in 1994, *J. Earthquake Prediction Res.*, 6, (3), 400–419, 1997.
- Zakharova A., S. Poigina, E. Rogozhin, and O. Starovoit, Earthquakes in Eurasia in 1995, *J. Earthquake Prediction Res.*, 7, (2), 196–214, 1998.
- Zlobin, T. K., *Seismological Constraints on the Structure of the Crust and Upper Mantle of the Kurile Island Arc*, Vladivostok, 1987.

(Received August 16, 2001)